

ON THE FEASIBILITY OF CROSS-TASK TRANSFER WITH MODEL-BASED REINFORCEMENT LEARNING

Yifan Xu^{1*}, Nicklas Hansen^{1*}, Zirui Wang¹, Yung-Chieh Chan¹

Hao Su¹, Zhuowen Tu¹

¹ University of California San Diego

ABSTRACT

Reinforcement Learning (RL) algorithms can solve challenging control problems directly from image observations, but they often require millions of environment interactions to do so. Recently, model-based RL algorithms have greatly improved sample-efficiency by concurrently learning an internal model of the world, and supplementing real environment interactions with imagined rollouts for policy improvement. However, learning an effective model of the world from scratch is challenging, and in stark contrast to humans that rely heavily on world understanding and visual cues for learning new skills. In this work, we investigate whether internal models learned by modern model-based RL algorithms can be leveraged to solve new, distinctly different tasks faster. We propose Model-Based **Cross-Task Transfer (XTRA)**, a framework for sample-efficient online RL with scalable pretraining and finetuning of learned world models. By offline multi-task pretraining and online cross-task finetuning, we achieve substantial improvements on the Atari100k benchmark over a baseline trained from scratch; we improve mean performance of model-based algorithm EfficientZero by 23%, and by as much as 71% in some instances. Project page: <https://nicklashansen.github.io/xtra>.

1 INTRODUCTION

Reinforcement Learning (RL) has achieved great feats across a wide range of areas, most notably game-playing (Mnih et al., 2013; Silver et al., 2016; Berner et al., 2019; Cobbe et al., 2020). However, traditional RL algorithms often suffer from poor sample-efficiency and require millions (or even billions) of environment interactions to solve tasks – especially when learning from high-dimensional observations such as images. This is in stark contrast to humans that have a remarkable ability to quickly learn new skills despite very limited exposure (Dubey et al., 2018). In an effort to reliably benchmark and improve the sample-efficiency of image-based RL across a variety of problems, the Arcade Learning Environment (ALE; (Bellemare et al., 2013)) has become a long-standing challenge for RL. This task suite has given rise to numerous successful and increasingly sample-efficient algorithms (Mnih et al., 2013; Badia et al., 2020; Kaiser et al., 2020; Schrittwieser et al., 2020; Kostrikov et al., 2021; Hafner et al., 2021; Ye et al., 2021), notably most of which are model-based, *i.e.*, they learn a *model* of the environment.

Most recently, EfficientZero Ye et al. (2021) – a model-based RL algorithm – has demonstrated impressive sample-efficiency, surpassing human-level performance with as little as 2 hours of real-time game play in select Atari 2600 games from the ALE. This achievement is attributed – in part – to the algorithm concurrently learning an internal *model* of the environment from interaction, and using the learned model to *imagine* (simulate) further interactions for planning and policy improvement, thus reducing reliance on real environment interactions for skill acquisition. However, current RL

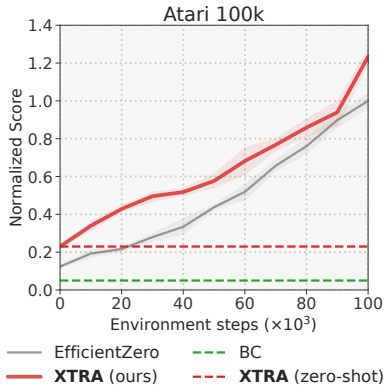


Figure 1. **Atari100k score**, normalized by mean EfficientZero performance at 100k environment steps across 10 games. Mean of 5 seeds; shaded area indicates 95% CIs.

* Equal contribution.

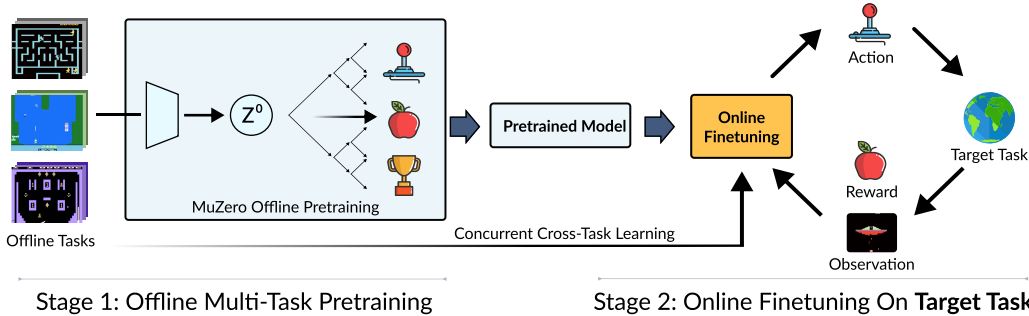


Figure 2. **Model-Based Cross-Task Transfer (XTRA)**. Our framework consists of two stages: (1) an *offline multi-task pretraining* stage where a single world model learns to solve diverse pretraining tasks, and (2) an *online finetuning* stage where the world model is jointly finetuned on a target task (with data collected by online interaction) in addition to the pretraining tasks (offline data).

algorithms – including EfficientZero – are still predominantly assumed to learn both perception, model, and skills *tabula rasa* (from scratch) for each new task. On the contrary, humans rely heavily on prior knowledge and visual cues when learning new skills. For example, a study found that human players easily pick up on visual cues about game mechanics and objectives when exposed to a video game for the very first time, and that human performance is severely degraded if such cues are removed or conflict with prior experiences (Dubey et al., 2018).

In related areas such as computer vision and natural language processing, large-scale unsupervised/self-supervised/supervised pretraining on large-scale datasets (Devlin et al., 2019; Brown et al., 2020; Li et al., 2022; Radford et al., 2021; Chowdhery et al., 2022) has emerged as a powerful framework for solving numerous downstream tasks with few samples (Alayrac et al., 2022). This pretraining paradigm has recently been extended to visuo-motor control in various forms, e.g., by leveraging *frozen* (no finetuning) pretrained representations (Xiao et al., 2022; Parisi et al., 2022) or by finetuning in a supervised setting (Reed et al., 2022; Lee et al., 2022). However, the success of finetuning for *online RL* has mostly been limited to same-task initialization of model-free policies from offline datasets (Wang et al., 2022; Zheng et al., 2022), or adapting policies to novel instances of a given task (Mishra et al., 2017; Julian et al., 2020; Hansen et al., 2021a), with prior work citing high-variance objectives and catastrophic forgetting as the main obstacles to finetuning representations with RL (Bodnar et al., 2020; Xiao et al., 2022).

In this work, we explore whether such positive transfer can be induced with current model-based RL algorithms in an *online RL* setting, and across *markedly distinct* tasks. Specifically, we seek to answer the following questions: *when* and *how* can a model-based RL algorithm such as EfficientZero benefit from pretraining on a diverse set of tasks? We base our experiments on the ALE due to cues that are easily identifiable to humans despite great diversity in tasks, and identify two key ingredients – cross-task finetuning and task alignment – for model-based adaptation that improve sample-efficiency substantially compared to models learned *tabula rasa*. In comparison, we find that a naïve treatment of the finetuning procedure as commonly used in supervised learning (Pan & Yang, 2010; Doersch et al., 2015; He et al., 2020; Reed et al., 2022; Lee et al., 2022) is found to be unsuccessful or outright *harmful* in an RL context.

Based on our findings, we propose Model-Based **Cross-Task Transfer (XTRA)**, a framework for sample-efficient online RL with scalable pretraining and finetuning of learned world models using extra, auxiliary data from other tasks. Concretely, our framework consists of two stages: (i) *offline multi-task pretraining* of a world model on an offline dataset from m diverse tasks, a (ii) *finetuning* stage where the world model is jointly finetuned on a *target task* in addition to the m offline tasks. By leveraging offline data both in pretraining and finetuning, XTRA overcomes the challenges of catastrophic forgetting. To prevent harmful interference from certain offline tasks, we adaptively re-weight gradient contributions in an unsupervised manner based on similarity to the target task.

We evaluate our method and a set of strong baselines extensively across 14 Atari 2600 games from the Atari100k benchmark (Kaiser et al., 2020) that require algorithms to be extremely sample-efficient. We find that XTRA improves sample-efficiency substantially across most tasks, improving mean and median performance of EfficientZero by 23% and 25%, respectively.

2 BACKGROUND

Problem setting. We model image-based agent-environment interaction as an episodic Partially Observable Markov Decision Process (POMDP; Kaelbling et al. (1998)) defined by the tuple $\mathcal{M} = \langle \mathcal{O}, \mathcal{A}, \mathcal{P}, \rho, r, \gamma \rangle$, where \mathcal{O} is the observation space (pixels), \mathcal{A} is the action space, $\mathcal{P}: \mathcal{O} \times \mathcal{A} \mapsto \mathcal{O}$ is a transition function, ρ is the initial state distribution, $r: \mathcal{O} \times \mathcal{A} \mapsto \mathbb{R}$ is a scalar reward function, and $\gamma \in [0, 1)$ is a discount factor. As is standard practice in ALE (Bellemare et al., 2013), we convert \mathcal{M} to a fully observable Markov Decision Process (MDP; Bellman (1957)) by approximating state $\mathbf{s}_t \in \mathcal{S}$ at time t as a stack of frames $\mathbf{s}_t \doteq \{o_t, o_{t-1}, o_{t-2}, \dots\}$ where $o \in \mathcal{O}$ (Mnih et al., 2013), and redefine \mathcal{P}, ρ, r to be functions of \mathbf{s} . Our goal is then to find a (neural) policy $\pi_\theta(\mathbf{a}|\mathbf{s})$ parameterized by θ that maximizes discounted return $\mathbb{E}_{\pi_\theta}[\sum_{t=1}^T \gamma^t r(\mathbf{s}_t, \mathbf{a}_t)]$ where $\mathbf{a}_t \sim \pi_\theta(\mathbf{a}|\mathbf{s})$, $\mathbf{s}_t \sim \mathcal{P}(\mathbf{s}_t, \mathbf{a}_t)$, $\mathbf{s}_0 \sim \rho$, and T is the episode horizon. For clarity, we denote all parameterization by θ throughout this work. To obtain a good policy from minimal environment interaction, we learn a "world model" from interaction data and use the learned model for action search. Define \mathcal{M} as the *target task* that we aim to solve. Then, we seek to first obtain a good parameter initialization θ that allows us to solve task \mathcal{M} using fewer interactions (samples) than training from scratch, *i.e.*, we wish to improve the *sample-efficiency* of online RL. We do so by first pretraining the model on an *offline* (fixed) dataset that consists of transitions $(\mathbf{s}, \mathbf{a}, r, \mathbf{s}')$ collected by unknown behavior policies in m environments $\{\hat{\mathcal{M}}^i \mid \hat{\mathcal{M}}^i \neq \mathcal{M}, 1 \leq i \leq m\}$, and then *finetune* the model by online interaction on the target task.

EfficientZero (Ye et al., 2021) is a model-based RL algorithm based on MuZero (Schrittwieser et al., 2020) that learns a discrete-action latent dynamics model from environment interactions, and selects actions by lookahead via Monte Carlo Tree Search (MCTS; (Abramson, 1987; Coulom, 2006; Silver et al., 2016)) in the latent space of the model. Figure 3 provides an overview of the three main components of the MuZero algorithm: a representation (encoder) h_θ , a dynamics (transition) function g_θ , and a prediction head f_θ . Given an observed state \mathbf{s}_t , EfficientZero projects the state to a latent representation $\mathbf{z}_t = h_\theta(\mathbf{s}_t)$, and predicts future latent states \mathbf{z}_{t+1} and instantaneous rewards r_t using an action-conditional latent dynamics function $\mathbf{z}_{t+1}, r_t = g_\theta(\mathbf{z}_t, \mathbf{a}_t)$. For each latent state, a prediction network f_θ estimates a probability distribution \hat{p} over (valid) actions $\mathbf{a} \in \mathcal{A}$, as well as the expected state value \hat{v} of the given state, *i.e.*, $\hat{v}_t, \hat{p}_t = f_\theta(\mathbf{z}_t)$.

Intuitively, h_θ and g_θ allow EfficientZero to search for actions entirely in its latent space before executing actions in the real environment, and f_θ predicts quantities that help guide the search towards high-return action sequences. Concretely, \hat{v} provides a return estimate for nodes at the lookahead horizon (as opposed to truncating the cumulative sum of expected rewards) and \hat{p} provides an action distribution prior that helps guide the search. EfficientZero improves the sample-efficiency of MuZero by introducing additional auxiliary losses during training. We adopt EfficientZero as our backbone model and learning algorithm, but emphasize that our framework is applicable to most model-based algorithms, including those for continuous action spaces (Hafner et al., 2019a; Hansen et al., 2022).

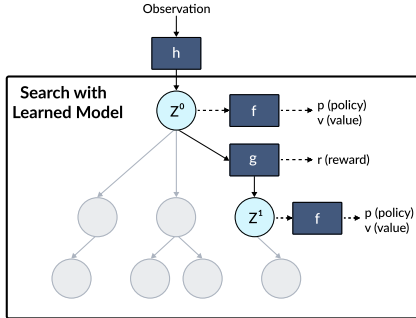


Figure 3. **MuZero/EfficientZero** combines MCTS with a learned representation network (h), latent dynamics function (g), and prediction heads (f).

3 MODEL-BASED CROSS-TASK TRANSFER

We propose Model-Based **Cross-Task Transfer** (**XTRA**), a two-stage framework for offline multi-task pretraining and cross-task transfer of learned world models by finetuning with online RL. Specifically, we first pretrain a world model on offline data from a set of diverse pretraining tasks, and then iteratively finetune the pretrained model on data from a *target* task collected by online interaction. In the following, we introduce each of the two stages – pretraining and finetuning – in detail.

3.1 OFFLINE MULTI-TASK PRETRAINING

In this stage, we aim to learn a single world model with general perceptive and dynamics priors across a diverse set of offline tasks. We emphasize, however, that the goal of pretraining is not to obtain a

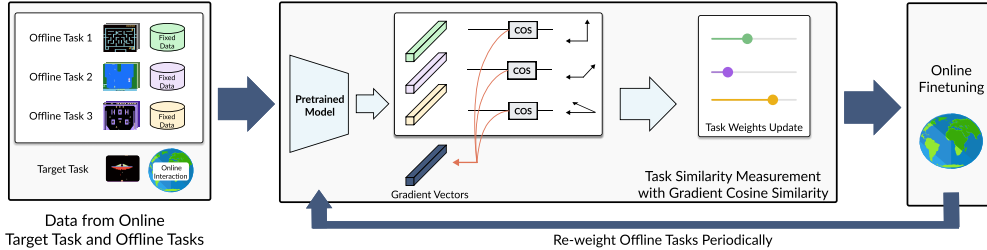


Figure 4. Concurrent Cross-Task Finetuning (Stage 2). Overview of our approach to online finetuning. We iteratively collect data for a target task by online interaction, and jointly finetune the model on data from the target task as well as offline data for each of the pretraining tasks. While this mitigates catastrophic forgetting, not all pretraining tasks are beneficial. Therefore, we periodically re-weight gradient contributions based on gradient cosine similarity to the target task.

truly generalist agent, but rather to learn a good initialization for finetuning to unseen tasks. Learning a single RL agent for a diverse set of tasks is however a difficult in practice, which is only exacerbated by extrapolation errors due to the offline RL setting (Kumar et al., 2020). To address the challenge of multi-task learning, we propose to pretrain the model following a *student-teacher* training setup, where *teacher* models are trained separately by offline RL for each task, and then distilled into a single multi-task model using a novel instantiation of the MuZero Reanalyze (Schrittwieser et al., 2021) algorithm.

For each pretraining task we assume access to a fixed dataset $\{\hat{\mathcal{D}}^i \mid 1 \leq i \leq m\}$ that consists of trajectories from an unknown (and potentially sub-optimal) behavior policy. Importantly, we do *not* make any assumptions about the quality or the source of trajectories in the dataset, *i.e.*, we do not assume datasets to consist of expert trajectories. We first train individual EfficientZero *teacher* models on each dataset for a fixed number of iterations in a single-task (offline) RL setting, resulting in m *teacher* models $\{\hat{\pi}_{\psi}^i \mid 1 \leq i \leq m\}$. After training, each *teacher* model $\hat{\pi}_{\psi}^i$ has learned to produce task-specific quantities $(\hat{\pi}, \hat{u}, \hat{z})$ for a given game $\hat{\mathcal{M}}^i$. Next, we learn a *multi-task student* model $\hat{\pi}_{\theta}$ by distilling the task-specific teachers into a single model. Specifically, we optimize the student policy by sampling data uniformly from all pretraining tasks, and generate value/policy targets using the respective teacher models rather than bootstrapping from student predictions as commonly done in the (single-task) MuZero Reanalyze algorithm. This step can be seen as learning multiple tasks simultaneously with direct supervision by distilling predictions from multiple teachers’ into a single model. Empirically, we find this to be a key component in scaling up the number of pretraining tasks. Although teacher models may not be optimal depending on the provided offline datasets, we find that they provide stable (due to fixed parameters during distillation) targets of sufficiently good quality. The simpler alternative – training a multi-task model on all m pretraining tasks simultaneously using RL is found to not scale beyond a couple of tasks in practice, as we will demonstrate our experiments in Appendix C. After distilling teacher models into the multi-task student model, we now have a single set of pretrained parameters that can be used for finetuning to a variety of tasks via online interaction, which we introduce in the following section.

3.2 ONLINE FINETUNING ON A TARGET TASK

In this stage, we iteratively interact with a target task (environment) to collect interaction data, and finetune the pretrained model on data from the target task. However, we empirically observe that directly finetuning the pretrained model often leads to catastrophic forgetting, and consequently poor performance on the target task. To overcome this challenge, we retain offline data from the pretraining stage, and concurrently finetune the model on both data from the target task, as well as data from the pretraining tasks. While this procedure addresses catastrophic forgetting, interference between the target task and certain pretraining tasks can be harmful for the sample-efficiency during online RL. As a solution, gradient contributions from offline tasks are periodically re-weighted in an unsupervised manner based on their similarity to the target task.

At each training step t , we jointly optimize the target online task \mathcal{M} and m offline (auxiliary) tasks $\{\hat{\mathcal{M}}^i \mid \hat{\mathcal{M}}^i \neq \mathcal{M}, 1 \leq i \leq m\}$ that were used during the *offline multi-task pretraining* stage. Our

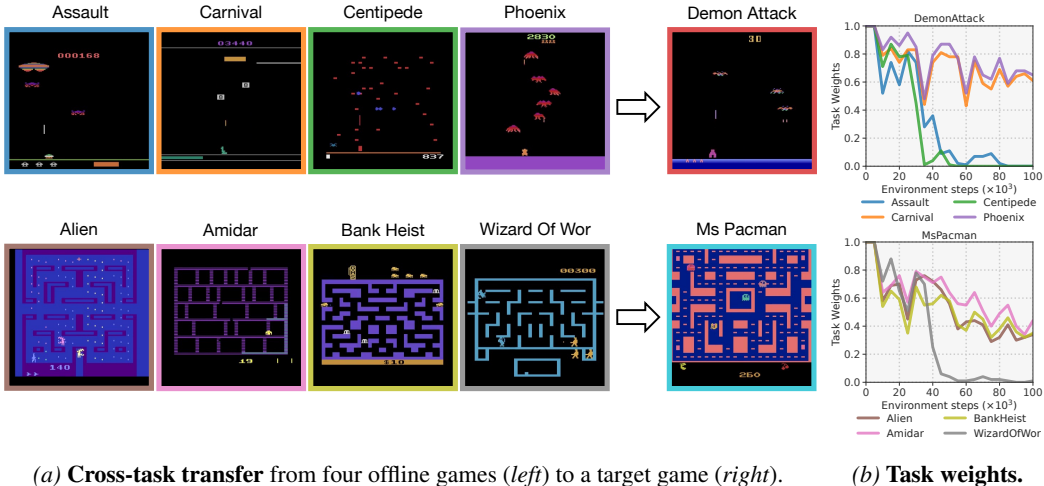


Figure 5. **Visualization of Concurrent Cross-Task Learning.** (a) A world model is concurrently finetuned on a target game as well as four offline games. (b) Task weights for each offline game are periodically updated based on their gradient similarity to two target games (DemonAttack/MsPacman).

online finetuning objective is defined as:

$$\mathcal{L}_t^{\text{adapt}}(\theta) = \mathcal{L}_t^{\text{ez}}(\mathcal{M}) + \sum_i \eta^i \mathcal{L}_t^{\text{ez}}(\hat{\mathcal{M}}^i) \quad (1)$$

where \mathcal{L}^{ez} is the ordinary (single-task) EfficientZero objective (see Appendix A), and η^i are dynamically (and independently) updated task weights for each of the m pretraining tasks. The target task loss term maintains a constant task weight of 1.

In order to dynamically re-weight task weights η^i throughout the training process, we break down the total number of environment steps (*i.e.*, 100k in our experiments) into even T -step cycles (intervals). Within each cycle, we spend first N -steps to compute an updated η^i corresponding to each offline task $\hat{\mathcal{M}}^i$. The new η^i will then be fixed during the remaining $T - N$ steps in the current cycle and the first N steps in the next cycle. We dynamically assign the task weights by measuring the “relevance” between each offline task $\hat{\mathcal{M}}^i$ and the (online) target task \mathcal{M} . Inspired by the conflicting gradients measurement for multi-task learning in (Yu et al., 2020), we compute the cosine similarity between loss gradients $\hat{\mathcal{G}}_n^i$ from $\mathcal{L}_n^{\text{ez}}(\hat{\mathcal{M}}^i)$ and \mathcal{G}_n from $\mathcal{L}_n^{\text{ez}}(\mathcal{M})$ given by

$$\text{Sim}(\hat{\mathcal{M}}^i, \mathcal{M}) = \frac{\hat{\mathcal{G}}_n^i \cdot \mathcal{G}_n}{\|\hat{\mathcal{G}}_n^i\| \|\mathcal{G}_n\|} \quad (2)$$

Within the N -step update, we maintain a task-specific counter s^i and the new task weights η^i can be reset by $\eta^i = \frac{s^i}{N}$ at the beginning of each every T -cycle following the procedure stated in Appendix B. Concretely, $\text{Sim}(\hat{\mathcal{M}}^i, \mathcal{M})$ measures the angle between two task gradients $\hat{\mathcal{G}}_n^i$ and \mathcal{G}_n . Intuitively, we aim to (approximately) prevent gradient contributions from the offline tasks from conflicting with the gradient update direction for the target task by regulating offline tasks objectives with task weights η . While re-weighting task weights at every gradient update would result in the least amount of conflicting gradients, it is prohibitively costly to do so in practice. However, we empirically find the cosine similarity of task gradients to be strongly correlated in time, *i.e.*, the cosine similarity does not change much between consecutive gradient steps. By instead updating task weights every N steps, our proposed technique mitigates gradient conflicts at a negligible computational cost in contrast to the compute-intensive gradient modification method proposed in (Yu et al., 2020).

4 EXPERIMENTS

We evaluate our method and baselines on **14** games (tasks) from the limited-interaction Atari 100k benchmark (Kaiser et al., 2020) where only 100k environment steps are permitted. We provide an implementation of our method at <https://github.com/mlpc-ucsd/XTRA>. Through experimental evaluation, we seek to answer the following three questions:

Table 1. Atari100k benchmark results (similar pretraining tasks). Methods are evaluated at 100k environment steps. For each game, XTRA is first pretrained on all 4 other games from the same category. Our main result is highlighted. We also include three ablations that remove (i) cross-task optimization in finetuning (only online RL), (ii) the pretraining stage (random initialization), and (iii) task re-weighting (constant weights of 1). We also include zero-shot performance of our method for target tasks in comparison to behavioral cloning. Mean of 5 seeds and 32 evaluation episodes.

Category	Game	Efficient Zero	Efficient Zero-L	XTRA (Ours)	Ablations (XTRA)			Zero-Shot	
					w.o. cross-task	w.o. pretraining	w.o. task weights	BC	XTRA (Ours)
<i>Shooter</i>	Assault	1027.1	1041.6	1294.6	1246.4	1257.5	1164.2	0.0	92.8
	Carnival	3022.1	2784.3	3860.9	3544.4	2370.0	3071.6	93.75	719.3
	Centipede	3322.7	2750.7	5681.4	3833.2	6322.7	5484.1	162.2	1206.8
	Demon Attack	11523.0	4691.0	14140.9	6381.5	9486.8	51045.9	73.8	113.6
	Phoenix	10954.9	3071.0	14579.8	10797.3	9010.6	22873.9	0.0	8073.4
	Mean Improvement	1.00	0.69	1.36	1.02	1.11	2.06	0.02	0.29
	Median Improvement	1.00	0.83	1.28	1.15	0.82	1.65	0.01	0.24
<i>Maze</i>	Alien	695.0	641.5	954.8	722.8	703.6	633.6	108.1	294.1
	Amidar	109.7	84.2	90.2	121.8	70.8	69.7	0.0	5.2
	Bank Heist	246.1	244.5	304.9	280.1	225.1	261.4	0.0	7.3
	Ms Pacman	1281.4	1172.8	1459.7	1011.1	1122.6	809.2	147.6	448.9
	Wizard Of Wor	1033.1	928.8	985.0	1246.1	654.4	263.5	100.0	9.4
	Mean Improvement	1.00	0.90	1.11	1.06	0.82	0.70	0.07	0.17
	Median Improvement	1.00	0.92	1.14	1.11	0.88	0.64	0.10	0.05
<i>Overall</i>	Mean Improvement	1.00	0.79	1.23	1.04	0.96	1.38	0.05	0.23
	Median Improvement	1.00	0.91	1.25	1.12	0.85	1.04	0.02	0.16

- How does our proposed framework compare to alternative pretraining and online RL approaches with *limited* online interaction from the target task?
- How do the individual components of our framework influence its success?
- When can we empirically expect finetuning to be successful?

Experimental setup. We base our architecture and backbone learning algorithm on EfficientZero (Ye et al., 2021) and focus our efforts on the pretraining and finetuning aspects of our problem setting. We consider EfficientZero with two different network sizes to better position our results: (i) the same network architecture as in the original EfficientZero implementation which we simply refer to as **EfficientZero**, and (ii) a larger variant with 4 times more parameters in the representation network (denoted **EfficientZero-L**). We use the EfficientZero-L variant as the default network for our framework through our experiments, unless stated otherwise. However, we find that our EfficientZero baseline generally does not benefit from a larger architecture, and we thus include both variants for a fair comparison. We experiment with cross-task transfer on three subsets of tasks: tasks that share *similar* game mechanics (for which we consider two *Shooter* and *Maze* categories), and tasks that have no discernible properties in common (referred to as *Diverse*). We measure performance on individual Atari games by absolute scores, and also provide aggregate results as measured by mean and median scores across games, normalized by either human performance or EfficientZero performance at 100k environment steps. All of our results are averaged across 5 random seeds to ensure reliability. See Appendix E for more details.

Baselines. We compare our method against 7 prior methods for online RL that represent the state-of-the-art on the Atari100k benchmark (including EfficientZero), as well as a multi-task behavior cloning policy trained on the full pretraining dataset, and a set of ablations that include EfficientZero with several different model sizes and pretraining/finetuning schemes. The former baselines serve to position our results with respect to the state-of-the-art, and the latter baselines and ablations serve to shed light on the key ingredients for successful multi-task pretraining and finetuning.

4.1 RESULTS & DISCUSSION

We introduce our results as they relate to each of our three questions, and discuss our main findings.

1. How does our proposed framework compare to alternative pretraining and online RL approaches with limited online interaction from the target task?

Tasks that share similar game mechanics. We first investigate the feasibility of finetuning models that are pretrained on games with *similar* mechanics. We select 5 shooter games and 5 maze games for

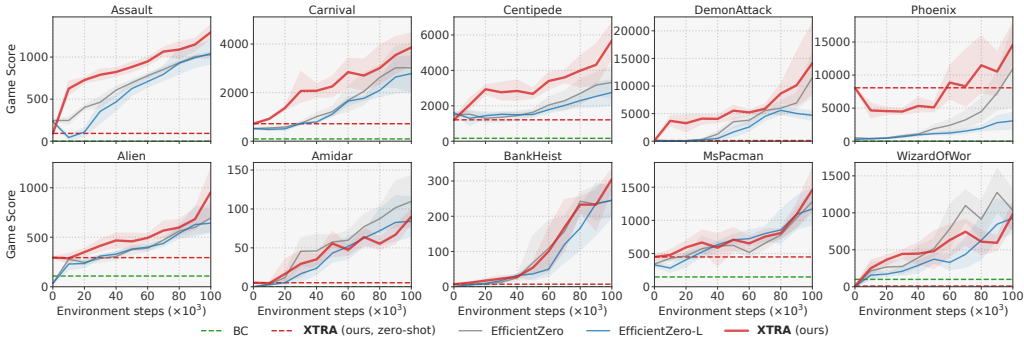


Figure 6. Atari100k benchmark results (similar pretraining tasks). We report unnormalized scores, aggregated across 5 seeds per game. Shaded area indicates 95% confidence intervals.

Table 2. Atari100k benchmark results (diverse pretraining tasks). XTRA results use the same set of pretrained model parameters obtained by offline pretraining on 8 diverse games. Mean of 5 seeds each with 32 evaluation episodes. Our result is highlighted. All other results are adopted from EfficientZero (Ye et al., 2021). We also report human-normalized mean and median scores.

Game	XTRA (Ours)	EfficientZero	Random	Human	SimPLe	OTRainbow	CURL	DrQ	SPR	MuZero
Assault	1742.2	1263.1	222.4	742.0	527.2	351.9	600.6	452.4	571.0	500.1
BattleZone	14631.25	13871.2	2360.0	37187.5	5184.4	4060.6	14870.0	12954.0	16651.0	7687.5
Hero	10631.8	9315.9	1027.0	30826.4	2656.6	6458.8	6279.3	3736.3	7019.2	3095.0
Krull	7735.8	5663.3	1598.0	2665.5	4539.9	3277.9	4229.6	4018.1	3688.9	4890.8
Seaquest	749.5	1100.2	68.4	42054.7	683.3	286.9	384.5	301.2	583.1	208.0
Normed Mean	1.87	1.29	0.0	1.0	0.70	0.41	0.75	0.62	0.65	0.77
Normed Median	0.35	0.33	0.0	1.0	0.08	0.18	0.36	0.30	0.41	0.15

this experiment. Results for our method, baselines, and a set of ablations on the Atari100k benchmark are shown in Table 1. For completeness, we also provide learning curves in Figure 6. We find that pretraining improves sample-efficiency substantially across most tasks, improving mean and median performance of EfficientZero by **23%** and **25%**, respectively, overall. Interestingly, XTRA also had a notable zero-shot ability compared to a multi-game behavior cloning baseline that is trained on the same offline dataset. We also consider three ablations: (1) **XTRA without cross-task**: a variant of our method that naively finetunes the pretrained model without any additional offline data from pretraining tasks during finetuning, (2) **XTRA without pretraining**: a variant that uses our concurrent cross-task learning (*i.e., leverages offline data during finetuning*) but is initialized with random parameters (no pretraining), and finally (3) **XTRA without task weights**: a variant that uses constant weights of 1 for all task loss terms during finetuning. We find that XTRA achieves extremely high performance on 2 games (DemonAttack and Phoenix) without dynamic task weights, improving over EfficientZero by as much as **343%** on DemonAttack. However, its median performance is overall low compared to our default variant that uses dynamic weights. We conjecture that this is because some (combinations of) games are more susceptible to gradient conflicts than others.

Tasks with diverse game mechanics. We now consider a more diverse set of pretraining and target games that have no discernible properties in common. Specifically, we use the following tasks for pretraining: Carnival, Centipede, Phoenix, Pooyan, Riverraid, VideoPinball, WizardOfWor, and YarsRevenge, and evaluate our method on 5 tasks from Atari100k. Results are shown in Table 2. We find that XTRA advances the state-of-the-art in a majority of tasks on the Atari100k benchmark, and achieve a mean human-normalized score of **187%** vs. **129%** for the previous SOTA, EfficientZero. This suggests that, while task similarity may play a role in the success of XTRA, the algorithmic advances of our proposed frames are a bigger factor in the strong empirical performance.

2. How do the individual components of our framework influence its success?

A deeper look at task relevance. While our previous experiments established that XTRA benefits from pretraining even when games are markedly different, we now seek to better quantify the importance of task relevance. We compare the online finetuning performance of XTRA in two different settings: (1) pretraining on 4 shooter games and finetuning to 5 new shooter games, and (2) pretraining on 4 maze games and finetuning to the same 5 shooter games. Aggregate results across

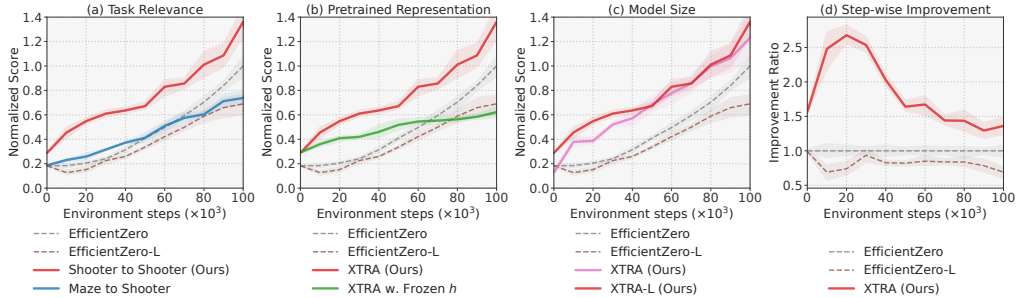


Figure 7. **Ablations.** (a) importance of task relevance, (b) finetuning vs. using a frozen pretrained representation, (c) model size (# parameters), and (d) improvement over baseline as a function of environment steps. Results are aggregate scores across 5 games and 5 random seeds.

all 5 target tasks are shown in Figure 7 (a). Unsurprisingly, we observe that offline pretraining and concurrently learning from other shooter games significantly benefit the online target shooter games through training, with particularly large gains early in training. On the contrary, pretraining on maze games and finetuning to shooter games show similar performance compared to EfficientZero trained from scratch. This result indicates that (1) selecting pretraining tasks that are relevant to the target task is key to benefit from pretraining, and (2) in the extreme case where there are *no* pretraining tasks relevant to the target task, finetuning with XTRA generally does not harm the online RL performance since it can automatically assign small weights to the pretraining tasks.

Which components transfer in model-based RL? Next, we investigate which model component(s) are important to the success of cross-task transfer. We answer this question by only transferring a subset of the different model components – representation h , dynamics function g , and prediction head f – to the online finetuning stage and simply using a random initialization for the remaining components. Results are shown in Figure 8. Interestingly, we find that only transferring the pretrained representation h to the online RL stage only improves slightly over learning from scratch, especially in the early stages of online RL. In comparison, loading both the pretrained representation *and* dynamics function accounts for the majority of the gains in XTRA, whereas loading the prediction heads has no significant impact on sample-efficiency (but matters for zero-shot performance). We conjecture that this is because learning a good dynamics function is relatively more difficult from few samples than learning a *task-specific* visual representation, and that the prediction head accounts for only a small amount of the overall parameters in the model. Finally, we hypothesize that the visual representation learned during pretraining will be susceptible to distribution shifts as it is transferred to an unseen target task. To verify this hypothesis, we consider an additional experiment where we transfer all components to new tasks, but *freeze* the representation h during finetuning, *i.e.*, it remains fixed. Results are shown in Figure 7 (b). We find that, although this variant of our framework improves over training from scratch in the early stages of training, the frozen representation eventually hinders the model from converging to a good model, which is consistent with observations made in model-free RL (Wang et al., 2022; Ze et al., 2022).

Scaling model size. In this experiment, we investigate whether XTRA benefits from larger model sizes. Since dynamics network g and prediction network f are used in MCTS search, increasing the parameter counts for these two networks would increase inference/training time complexity significantly. However, increasing the size of the representation network h has a relatively small impact on overall inference/training time (see Figure 3 for reference). We compare the performance of our method and EfficientZero trained from scratch with each of our two model sizes, the original EfficientZero architecture and a larger variant (denoted EfficientZero-L); results are shown in Figure 7 (c). We find that our default, larger variant of XTRA (denoted XTRA-L in the figure) is slightly better than the smaller model size. In comparison, EfficientZero-L, performs significantly worse than

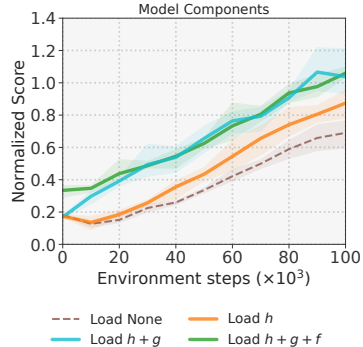


Figure 8. **Transferring model components.** Aggregated scores from 5 shooter games by loading parameters of select pretrained model components. Here, h , g , and f denote the representation, dynamics, and prediction networks respectively. Mean of 5 seeds; shading: 95% CIs.

the smaller variant of EfficientZero. This indicates that, unlike EfficientZero trained from scratch, XTRA is robust to model size and can potentially benefit from further scaling up the model size (along with more pretraining tasks) in the future.

Relative improvement vs. environment steps. Finally, we visualize the average improvement over EfficientZero throughout training in Figure 7 (d). Results show that XTRA is particularly useful in the early stages of training, *i.e.*, in an extremely limited data setting. We therefore envision that cross-task pretraining could benefit many real-world applications of RL, where environment interactions are typically constrained due to physical constraints.

3. When can we empirically expect finetuning to be successful?

We have demonstrated that model-based RL can benefit from cross-task transfer, both when the tasks are *similar* to the target task (Table 1), and when tasks are *diverse* (*i.e.*, dissimilar to the target task; Table 2). While transfer is more successful overall when tasks are similar (*e.g.*, shooter games that feature similar game mechanics), our proposed approach to finetuning is found to successfully reduce (potentially harmful) gradient contributions of dissimilar tasks as measured by gradient cosine similarity to the target game. Interestingly, we find that both the representation and dynamics networks benefit from pretraining despite differences in game mechanics (Figure 8), but that leveraging a *frozen* pretrained representation reduces sample-efficiency compared to finetuning. This finding confirms that (1) pretraining a model-based algorithm requires special considerations vs. pretraining a model-free method, and (2) the observation that a *frozen* representation generally is inferior to finetuning in model-free RL (Wang et al., 2022; Ze et al., 2022) also applies to model-based RL.

5 RELATED WORK

Pretrained representations are widely used to improve downstream performance in learning tasks with limited data or resources available, and have been adopted across a multitude of areas such as computer vision (Girshick et al., 2014; Doersch et al., 2015; He et al., 2020), natural language processing (Devlin et al., 2019; Brown et al., 2020), and audio (van den Oord et al., 2018). By first learning a good representation on a large dataset, the representation can quickly be finetuned with, *e.g.*, supervised learning on a small labelled dataset to solve a given task (Pan & Yang, 2010). For example, He et al. (2020) show that contrastive pretraining on a large, unlabelled dataset learns good features for ImageNet classification, and Brown et al. (2020) show that a generative model trained on large-scale natural language data can be used to solve unseen tasks given only a few examples. While this is a common paradigm for problems that can be cast as (self-)supervised learning problems, it has seen comparably little adoption in RL literature. This discrepancy is, in part, attributed to optimization challenges in RL (Bodnar et al., 2020; Hansen et al., 2021b; Xiao et al., 2022; Wang et al., 2022), as well as a lack of large-scale datasets that capture both the visual, temporal, and control-relevant (actions, rewards) properties of RL. In this work, we show that – despite these challenges – modern model-based RL algorithms can still benefit substantially from pretraining on multi-task datasets, but require a more careful treatment during finetuning.

Sample-efficient RL. Improving the sample-efficiency of visual RL algorithms is a long-standing problem and has been approached from many – largely orthogonal – perspectives, including representation learning (Kulkarni et al., 2019; Yarats et al., 2019; Srinivas et al., 2020; Schwarzer et al., 2021), data augmentation (Laskin et al., 2020; Kostrikov et al., 2021; Hansen et al., 2021b), bootstrapping from demonstrations (Zhan et al., 2020) or offline datasets (Wang et al., 2022; Zheng et al., 2022; Baker et al., 2022), using pretrained visual representations for model-free RL (Shah & Kumar, 2021; Xiao et al., 2022; Ze et al., 2022), and model-based RL (Finn & Levine, 2017; Nair et al., 2018; Hafner et al., 2019b; Kaiser et al., 2020; Schrittwieser et al., 2020; Hafner et al., 2021; Ye et al., 2021; Hansen et al., 2022; Seo et al., 2022). We choose to focus our efforts on sample-efficiency from the perspective of pretraining in a model-based context, *i.e.*, jointly learning perception *and* dynamics. Several prior works consider these problems independently from each other: Xiao et al. (2022) shows that model-free policies can be trained with a frozen pretrained visual backbone, and Seo et al. (2022) shows that learning a world model on top of features from a visual backbone pretrained with video prediction can improve model learning. Our work differs from prior work in that we show it is possible to pretrain *and* finetune both the representation *and* the dynamics using model-based RL.

Finetuning in RL. Gradient-based finetuning is a well-studied technique for adaptation in (predominantly model-free) RL, and has been used to adapt to either changes in visuals or dynamics (Mishra

et al., 2017; Yen-Chen et al., 2019; Duan et al., 2016; Julian et al., 2020; Hansen et al., 2021a; Bodnar et al., 2020; Wang et al., 2022; Ze et al., 2022), or task specification (Xie & Finn, 2021; Walke et al., 2022). For example, Julian et al. (2020) shows that a model-free policy for robotic manipulation can adapt to changes in lighting and object shape by finetuning via rewards on a mixture of data from the new and old environment, and recover original performance in less than 800 trials. Similarly, Hansen et al. (2021a) shows that model-free policies can (to some extent) also adapt to small domain shifts by self-supervised finetuning within a single episode. Other works show that pretraining with offline RL on a dataset from a specific task improve sample-efficiency during online finetuning on the same task (Zheng et al., 2022; Wang et al., 2022). Finally, Lee et al. (2022) shows that offline multi-task RL pretraining via sequence modelling can improve offline finetuning on data from unseen tasks. Our approach is most similar to Julian et al. (2020) in that we finetune via rewards on a mixture of datasets. However, our problem setting is fundamentally different: we investigate whether *multi-task* pretraining can improve online RL on an *unseen* task across *multiple* axes of variation.

6 CONCLUSION

In this paper, we propose Model-Based **Cross-Task Transfer (XTRA)**, a framework for sample-efficient online RL with scalable pretraining and finetuning of learned world models using extra, auxiliary data from other tasks. We find that XTRA improves sample-efficiency substantially across most tasks, improving mean and median performance of EfficientZero by 23% and 25%, respectively, overall. As a feasibility study, we hope that our empirical analysis and findings on cross-task transfer with model-based RL will inspire further research in this direction.

Acknowledgements. This work is supported by NSF Award IIS-2127544 and gifts from Qualcomm AI. We thank Weirui Ye and Wenlong Huang for their helpful discussions.

REFERENCES

- Bruce D. Abramson. *The Expected-Outcome Model of Two-Player Games*. PhD thesis, 1987. AAI8827528.
- Jean-Baptiste Alayrac, Jeff Donahue, Pauline Luc, Antoine Miech, Iain Barr, Yana Hasson, Karel Lenc, Arthur Mensch, Katie Millican, Malcolm Reynolds, et al. Flamingo: a visual language model for few-shot learning. *arXiv preprint arXiv:2204.14198*, 2022.
- Adrià Puigdomènech Badia, Bilal Piot, Steven Kapturowski, Pablo Sprechmann, Alex Vitvitskyi, Daniel Guo, and Charles Blundell. Agent57: Outperforming the atari human benchmark. *ArXiv*, abs/2003.13350, 2020.
- Bowen Baker, Ilge Akkaya, Peter Zhokhov, Joost Huizinga, Jie Tang, Adrien Ecoffet, Brandon Houghton, Raul Sampedro, and Jeff Clune. Video pretraining (vpt): Learning to act by watching unlabeled online videos. *ArXiv*, abs/2206.11795, 2022.
- Marc G. Bellemare, Yavar Naddaf, Joel Veness, and Michael Bowling. The arcade learning environment: An evaluation platform for general agents (extended abstract). In *IJCAI*, 2013.
- Richard Bellman. A markovian decision process. *Journal of Mathematics and Mechanics*, 6(5): 679–684, 1957.
- Christopher Berner, Greg Brockman, Brooke Chan, Vicki Cheung, Przemyslaw Debiak, Christy Dennison, David Farhi, Quirin Fischer, Shariq Hashme, Christopher Hesse, Rafal Józefowicz, Scott Gray, Catherine Olsson, Jakub W. Pachocki, Michael Petrov, Henrique Pondé de Oliveira Pinto, Jonathan Raiman, Tim Salimans, Jeremy Schlatter, Jonas Schneider, Szymon Sidor, Ilya Sutskever, Jie Tang, Filip Wolski, and Susan Zhang. Dota 2 with large scale deep reinforcement learning. *ArXiv*, abs/1912.06680, 2019.
- Cristian Bodnar, Karol Hausman, Gabriel Dulac-Arnold, and Rico Jonschkowski. A geometric perspective on self-supervised policy adaptation. *ArXiv*, abs/2011.07318, 2020.

- Tom B. Brown, Benjamin Mann, Nick Ryder, Melanie Subbiah, Jared Kaplan, Prafulla Dhariwal, Arvind Neelakantan, Pranav Shyam, Girish Sastry, Amanda Aspell, Sandhini Agarwal, Ariel Herbert-Voss, Gretchen Krueger, T. J. Henighan, Rewon Child, Aditya Ramesh, Daniel M. Ziegler, Jeff Wu, Clemens Winter, Christopher Hesse, Mark Chen, Eric Sigler, Mateusz Litwin, Scott Gray, Benjamin Chess, Jack Clark, Christopher Berner, Sam McCandlish, Alec Radford, Ilya Sutskever, and Dario Amodei. Language models are few-shot learners. *ArXiv*, abs/2005.14165, 2020.
- Aakanksha Chowdhery, Sharan Narang, Jacob Devlin, Maarten Bosma, Gaurav Mishra, Adam Roberts, Paul Barham, Hyung Won Chung, Charles Sutton, Sebastian Gehrmann, et al. Palm: Scaling language modeling with pathways. *arXiv preprint arXiv:2204.02311*, 2022.
- Karl Cobbe, Christopher Hesse, Jacob Hilton, and John Schulman. Leveraging procedural generation to benchmark reinforcement learning. *ArXiv*, abs/1912.01588, 2020.
- Rémi Coulom. Efficient selectivity and backup operators in monte-carlo tree search. In *International conference on computers and games*, pp. 72–83. Springer, 2006.
- Jacob Devlin, Ming-Wei Chang, Kenton Lee, and Kristina Toutanova. Bert: Pre-training of deep bidirectional transformers for language understanding. *ArXiv*, abs/1810.04805, 2019.
- Carl Doersch, Abhinav Kumar Gupta, and Alexei A. Efros. Unsupervised visual representation learning by context prediction. *2015 IEEE International Conference on Computer Vision (ICCV)*, pp. 1422–1430, 2015.
- Yan Duan, John Schulman, Xi Chen, Peter L. Bartlett, Ilya Sutskever, and P. Abbeel. RL2: Fast reinforcement learning via slow reinforcement learning. *ArXiv*, abs/1611.02779, 2016.
- Rachit Dubey, Pulkit Agrawal, Deepak Pathak, Thomas L. Griffiths, and Alexei A. Efros. Investigating human priors for playing video games. In *ICML*, 2018.
- Chelsea Finn and Sergey Levine. Deep visual foresight for planning robot motion. *2017 IEEE International Conference on Robotics and Automation (ICRA)*, pp. 2786–2793, 2017.
- Ross B. Girshick, Jeff Donahue, Trevor Darrell, and Jitendra Malik. Rich feature hierarchies for accurate object detection and semantic segmentation. *2014 IEEE Conference on Computer Vision and Pattern Recognition*, pp. 580–587, 2014.
- Danijar Hafner, Timothy Lillicrap, Jimmy Ba, and Mohammad Norouzi. Dream to control: Learning behaviors by latent imagination. *arXiv preprint arXiv:1912.01603*, 2019a.
- Danijar Hafner, Timothy P. Lillicrap, Ian S. Fischer, Ruben Villegas, David R Ha, Honglak Lee, and James Davidson. Learning latent dynamics for planning from pixels. *ArXiv*, abs/1811.04551, 2019b.
- Danijar Hafner, Timothy P. Lillicrap, Mohammad Norouzi, and Jimmy Ba. Mastering atari with discrete world models. *ArXiv*, abs/2010.02193, 2021.
- Nicklas Hansen, Rishabh Jangir, Yu Sun, Guillem Alenyà, Pieter Abbeel, Alexei A. Efros, Lerrel Pinto, and Xiaolong Wang. Self-supervised policy adaptation during deployment. In *International Conference on Learning Representations (ICLR)*, 2021a.
- Nicklas Hansen, Hao Su, and Xiaolong Wang. Stabilizing deep q-learning with convnets and vision transformers under data augmentation. In *NeurIPS*, 2021b.
- Nicklas Hansen, Xiaolong Wang, and Hao Su. Temporal difference learning for model predictive control. In *ICML*, 2022.
- Kaiming He, Haoqi Fan, Yuxin Wu, Saining Xie, and Ross B. Girshick. Momentum contrast for unsupervised visual representation learning. *2020 IEEE/CVF Conference on Computer Vision and Pattern Recognition (CVPR)*, pp. 9726–9735, 2020.
- Ryan C. Julian, Benjamin Swanson, Gaurav S. Sukhatme, Sergey Levine, Chelsea Finn, and Karol Hausman. Efficient adaptation for end-to-end vision-based robotic manipulation. *ArXiv*, abs/2004.10190, 2020.

- Leslie Pack Kaelbling, Michael L. Littman, and Anthony R. Cassandra. Planning and acting in partially observable stochastic domains. *Artificial Intelligence*, 1998.
- Lukasz Kaiser, Mohammad Babaeizadeh, Piotr Milos, Blazej Osinski, Roy H. Campbell, K. Czechowski, D. Erhan, Chelsea Finn, Piotr Kozakowski, Sergey Levine, Ryan Sepassi, G. Tucker, and Henryk Michalewski. Model-based reinforcement learning for atari. *ArXiv*, abs/1903.00374, 2020.
- Ilya Kostrikov, Denis Yarats, and Rob Fergus. Image augmentation is all you need: Regularizing deep reinforcement learning from pixels. *ArXiv*, abs/2004.13649, 2021.
- Tejas D. Kulkarni, Ankush Gupta, Catalin Ionescu, Sebastian Borgeaud, Malcolm Reynolds, Andrew Zisserman, and Volodymyr Mnih. Unsupervised learning of object keypoints for perception and control. *ArXiv*, abs/1906.11883, 2019.
- Aviral Kumar, Aurick Zhou, G. Tucker, and Sergey Levine. Conservative q-learning for offline reinforcement learning. *ArXiv*, abs/2006.04779, 2020.
- Michael Laskin, Kimin Lee, Adam Stooke, Lerrel Pinto, P. Abbeel, and A. Srinivas. Reinforcement learning with augmented data. *ArXiv*, abs/2004.14990, 2020.
- Kuang-Huei Lee, Ofir Nachum, Mengjiao Yang, L. Y. Lee, Daniel Freeman, Winnie Xu, Sergio Guadarrama, Ian S. Fischer, Eric Jang, Henryk Michalewski, and Igor Mordatch. Multi-game decision transformers. *ArXiv*, abs/2205.15241, 2022.
- Chunyuan Li, Haotian Liu, Liunian Harold Li, Pengchuan Zhang, Jyoti Aneja, Jianwei Yang, Ping Jin, Yong Jae Lee, Houdong Hu, Zicheng Liu, et al. Elevater: A benchmark and toolkit for evaluating language-augmented visual models. *arXiv preprint arXiv:2204.08790*, 2022.
- Nikhil Mishra, Mostafa Rohaninejad, Xi Chen, and P. Abbeel. Meta-learning with temporal convolutions. *ArXiv*, abs/1707.03141, 2017.
- Volodymyr Mnih, Koray Kavukcuoglu, David Silver, Alex Graves, Ioannis Antonoglou, Daan Wierstra, and Martin Riedmiller. Playing atari with deep reinforcement learning. *arXiv preprint arXiv:1312.5602*, 2013.
- Ashvin Nair, Vitchyr H. Pong, Murtaza Dalal, Shikhar Bahl, Steven Lin, and Sergey Levine. Visual reinforcement learning with imagined goals. In *NeurIPS*, 2018.
- Sinno Jialin Pan and Qiang Yang. A survey on transfer learning. *IEEE Transactions on Knowledge and Data Engineering*, 22:1345–1359, 2010.
- Simone Parisi, Aravind Rajeswaran, Senthil Purushwalkam, and Abhinav Kumar Gupta. The unsurprising effectiveness of pre-trained vision models for control. In *ICML*, 2022.
- Alec Radford, Jong Wook Kim, Chris Hallacy, Aditya Ramesh, Gabriel Goh, Sandhini Agarwal, Girish Sastry, Amanda Askell, Pamela Mishkin, Jack Clark, et al. Learning transferable visual models from natural language supervision. In *International Conference on Machine Learning*, pp. 8748–8763, 2021.
- Scott Reed, Konrad Zolna, Emilio Parisotto, Sergio Gomez Colmenarejo, Alexander Novikov, Gabriel Barth-Maron, Mai Gimenez, Yury Sulsky, Jackie Kay, Jost Tobias Springenberg, Tom Eccles, Jake Bruce, Ali Razavi, Ashley D. Edwards, Nicolas Manfred Otto Heess, Yutian Chen, Raia Hadsell, Oriol Vinyals, Mahyar Bordbar, and Nando de Freitas. A generalist agent. *ArXiv*, abs/2205.06175, 2022.
- Julian Schrittwieser, Ioannis Antonoglou, Thomas Hubert, Karen Simonyan, L. Sifre, Simon Schmitt, Arthur Guez, Edward Lockhart, Demis Hassabis, Thore Graepel, Timothy P. Lillicrap, and David Silver. Mastering atari, go, chess and shogi by planning with a learned model. *Nature*, 2020.
- Julian Schrittwieser, Thomas K Hubert, Amol Mandhane, Mohammadamin Barekatain, Ioannis Antonoglou, and David Silver. Online and offline reinforcement learning by planning with a learned model. In A. Beygelzimer, Y. Dauphin, P. Liang, and J. Wortman Vaughan (eds.), *Advances in Neural Information Processing Systems*, 2021. URL <https://openreview.net/forum?id=HKtsGW-lNbw>.

- Max Schwarzer, Ankesh Anand, Rishab Goel, R. Devon Hjelm, Aaron C. Courville, and Philip Bachman. Data-efficient reinforcement learning with self-predictive representations. In *ICLR*, 2021.
- Younggyo Seo, Kimin Lee, Stephen James, and P. Abbeel. Reinforcement learning with action-free pre-training from videos. In *ICML*, 2022.
- Rutav Shah and Vikash Kumar. Rrl: Resnet as representation for reinforcement learning. *ArXiv*, abs/2107.03380, 2021.
- David Silver, Aja Huang, Christopher Maddison, Arthur Guez, Laurent Sifre, George Driessche, Julian Schrittwieser, Ioannis Antonoglou, Veda Panneershelvam, Marc Lanctot, Sander Dieleman, Dominik Grewe, John Nham, Nal Kalchbrenner, Ilya Sutskever, Timothy Lillicrap, Madeleine Leach, Koray Kavukcuoglu, Thore Graepel, and Demis Hassabis. Mastering the game of go with deep neural networks and tree search. *Nature*, 529:484–489, 01 2016. doi: 10.1038/nature16961.
- A. Srinivas, Michael Laskin, and P. Abbeel. Curl: Contrastive unsupervised representations for reinforcement learning. In *ICML*, 2020.
- Aäron van den Oord, Yazhe Li, and Oriol Vinyals. Representation learning with contrastive predictive coding. *ArXiv*, abs/1807.03748, 2018.
- Homer Walke, Jonathan Yang, Albert Yu, Aviral Kumar, Jędrzej Orbik, Avi Singh, and Sergey Levine. Don’t start from scratch: Leveraging prior data to automate robotic reinforcement learning. *ArXiv*, abs/2207.04703, 2022.
- Che Wang, Xufang Luo, Keith W. Ross, and Dongsheng Li. Vrl3: A data-driven framework for visual deep reinforcement learning. *ArXiv*, abs/2202.10324, 2022.
- Tete Xiao, Ilija Radosavovic, Trevor Darrell, and Jitendra Malik. Masked visual pre-training for motor control. *ArXiv*, abs/2203.06173, 2022.
- Annie Xie and Chelsea Finn. Lifelong robotic reinforcement learning by retaining experiences. *ArXiv*, abs/2109.09180, 2021.
- Denis Yarats, Amy Zhang, Ilya Kostrikov, Brandon Amos, Joelle Pineau, and Rob Fergus. Improving sample efficiency in model-free reinforcement learning from images. 2019.
- Weirui Ye, Shaohuai Liu, Thanard Kurutach, P. Abbeel, and Yang Gao. Mastering atari games with limited data. In *NeurIPS*, 2021.
- Lin Yen-Chen, Maria Bauza, and Phillip Isola. Experience-embedded visual foresight. In *Conference on Robot Learning*, 2019.
- Tianhe Yu, Saurabh Kumar, Abhishek Gupta, Sergey Levine, Karol Hausman, and Chelsea Finn. Gradient surgery for multi-task learning. *Advances in Neural Information Processing Systems*, 33: 5824–5836, 2020.
- Yanjie Ze, Nicklas Hansen, Yinbo Chen, Mohit Jain, and Xiaolong Wang. Visual reinforcement learning with self-supervised 3d representations. *arXiv preprint arXiv:2210.07241*, 2022.
- Albert Zhan, Philip Zhao, Lerrel Pinto, P. Abbeel, and Michael Laskin. A framework for efficient robotic manipulation. *ArXiv*, abs/2012.07975, 2020.
- Qinqing Zheng, Amy Zhang, and Aditya Grover. Online decision transformer. In *ICML*, 2022.

A EFFICIENTZERO OBJECTIVE

MuZero (Schrittwieser et al., 2020) learns to predict three quantities used in MCTS: (1) policy target π obtained from the visit count distribution of the MCTS, (2) instantaneous reward u from environment transitions, and (3) bootstrapped value target $z = \sum_{i=0}^{k-1} \gamma^i u^i + \gamma^k v_{t+k}$. EfficientZero (Ye et al., 2021) extends MuZero by adding a self-supervised consistency loss term, and predicts the cumulative sum of rewards instead of individual single-step rewards. Concretely, the EfficientZero objective for time step t and with a total of K unroll steps is given by

$$\mathcal{L}_t^{\text{ez}}(\theta) = \sum_{k=0}^K \underbrace{\|\mathcal{L}^r(u_{t+k}, \hat{r}_t^k)\|_2^2}_{\text{reward}} + \lambda_1 \underbrace{\|\mathcal{L}^p(\pi_{t+k}, \hat{p}_t^k)\|_2^2}_{\text{policy}} + \lambda_2 \underbrace{\|\mathcal{L}^v(z_{t+k}, \hat{v}_t^k)\|_2^2}_{\text{value}} + \lambda_3 \underbrace{\|\mathcal{L}^s(s_{t+1}, \hat{s}_{t+1})\|_2^2}_{\text{consistency}} + c \|\theta\| \quad (3)$$

where $\lambda_{1,3}$ and c are constant coefficients that balance the five terms. However, we note that our approach is agnostic to the specific choice of algorithm; we only include this additional discussion for completeness. We refer the reader to Ye et al. (2021) for more algorithmic details.

B PERIODIC TASK RE-WEIGHTING

Between each N -step update, we maintain a task-specific counter s^i for the i th task, and update the counter by Δs_n^i at each step n as follows:

$$\Delta s_n^i = \begin{cases} 1, & \text{if } \text{Sim}(\hat{\mathcal{M}}^i, \mathcal{M}) > 0.1 \\ 0, & \text{otherwise} \end{cases} \\ s^i = s^i + \Delta s_n^i. \quad (4)$$

At every N steps, the new task weights η^i are updated by $\eta^i = \frac{s^i}{N}$, and used in subsequent finetuning objectives according to Equation 1. In practice, we start task weight updates at 10k steps to ensure enough data from the online target task has been collected for a meaningful similarity measure. All task weights are initialized as 1 for the first 10k steps. Figure 5 shows task weights as a function of environment steps for two target games; additional results are provided in Figure 9.

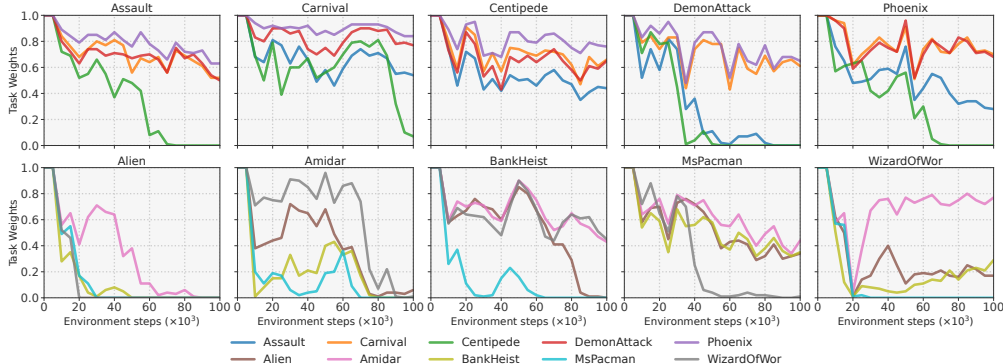


Figure 9. Periodic task re-weighting. We visualize task weights as a function of environment steps for each of our 10 tasks from Table 1. First row corresponds to *shooter* games and the bottom row corresponds to *maze* games. We evaluate task weights on all tasks from the same category except for the target task itself.

C DISTILLATION VS. MULTI-GAME OFFLINE RL

Our method learns a multi-game world model from offline data via distillation of task-specific world models trained with offline RL. An alternative way to obtain such a multi-game model would be to directly train a single world model on the multi-game dataset with offline RL. However, we find that learning such a model is difficult. A comparison between the two approaches on four different pretraining games is shown in Figure 10. We observe that multi-game offline RL (*green*) achieves low scores in all four pretraining games, whereas our world model obtained by distillation (*orange*) performs comparably to single-task world models (*blue*) in 3 out of 4 tasks.

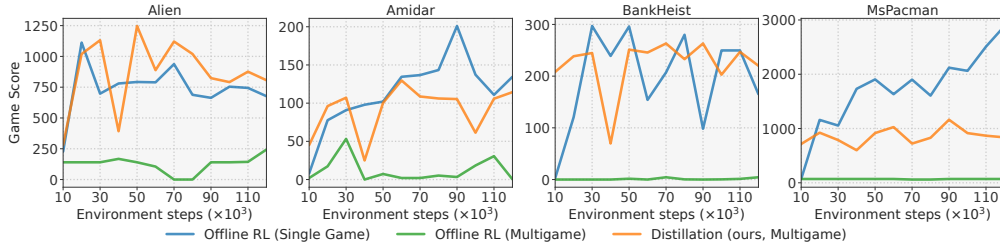


Figure 10. **Distillation vs. multi-game offline RL.** Results are shown on four pretraining tasks. Single-game models (*blue*) are trained via offline RL on each individual task, whereas results for multi-game offline RL (*green*) and our proposed distillation (*orange*) are obtained by evaluating a single set of pretraining parameters. Distillation nearly matches single-task performance.

D EFFECT OF MINI-BATCH SIZE

During online finetuning (stage 2), we finetune both with data from the target task, and data from the pretraining tasks. We maintain the same batch size (256) for the target task data as the non-pretraining baselines, but add additional data from the pretraining tasks with a 1:1 ratio. Thus, our effective batch size is $2\times$ that of the baselines. To verify that performance improvements stem from our pretraining (stage 1) and not the larger batch size, we compare our method to a variant of our EfficientZero-L baseline that uses a $2\times$ larger batch size (512). Results are shown in Figure 11. We do not observe any significant change in performance by doubling the batch size for the baseline. Thus, we conclude that a larger (effective) batch size is not the source of our performance gains, but rather our pretraining and inclusion of pretraining tasks during the online finetuning.

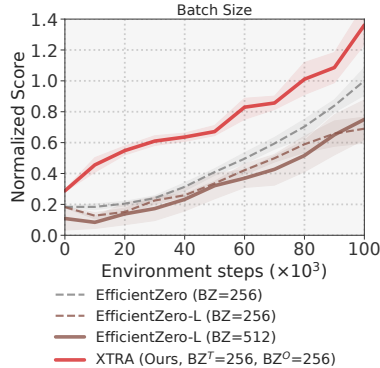


Figure 11. **Effect of mini-batch size (BZ).** For XTRA, we denote the batch size of the **T**arget task and **O**ffline tasks as BZ^T and BZ^O , respectively.

E SCORES FOR INDIVIDUAL SEEDS

Our results in Table 1 are aggregated across 5 seeds. In Table 3, we report game scores for each individual seed, as well as the mean, median, and standard deviation of game scores for each game. We also list random and human scores obtained from Badia et al. (2020), and calculate the Human Normalized Score based on the formula: $(\text{score}_{\text{agent}} - \text{score}_{\text{random}}) / (\text{score}_{\text{human}} - \text{score}_{\text{random}})$ as in prior work. To the best of our knowledge, there are no human performance results for the Carnival game, and we therefore exclude this game from the aggregate Human Normalized Mean and Median Scores computed in Table 3.

Table 3. **Scores for individual seeds.** Per-seed game scores for our method, a random behavior baseline, and human performance. We report both unnormalized and normalized scores (Human Normalized Scores), as well as their aggregate results. Random and human scores are obtained from Badia et al. (2020). We evaluate each random seed on 32 evaluation episodes at 100k steps.

Game	Game Score per Seed					Aggregated Metrics			References		Human Normed
	Seed 0	Seed 1	Seed 2	Seed 3	Seed 4	Mean	Median	Std	Random	Human	
Assault	1450.19	1356.53	1236.19	1215.12	1214.72	1294.55	1236.19	105.06	222.40	742.00	2.06
Carnival	3865.31	4867.50	4155.62	2601.88	3814.38	3860.94	3865.31	819.67	-	-	-
Centipede	7596.38	6179.25	5380.41	5300.03	3950.88	5681.39	5380.41	1336.58	2090.90	12017.00	0.36
DemonAttack	10470.78	8051.25	27574.06	8117.81	16490.47	14140.88	10470.78	8258.35	152.10	1971.00	7.69
Phoenix	20875.94	10988.44	10521.88	15803.44	14709.06	14579.75	14709.06	4198.81	761.40	7242.60	2.13
Alien	569.69	807.50	814.06	1388.12	1194.38	954.75	814.06	329.77	227.80	7127.70	0.11
Amidar	93.00	104.34	76.47	97.38	79.59	90.16	93.00	11.84	5.80	1719.50	0.05
BankHeist	303.12	316.56	270.62	270.00	364.06	304.88	303.12	38.83	14.20	753.10	0.39
MsPacman	1109.69	1960.00	1865.94	1228.44	1134.38	1459.69	1228.44	417.48	307.30	6951.60	0.17
WizardOfWor	1275.00	687.50	1056.25	990.62	915.62	985.00	990.62	213.62	563.50	4756.50	0.10
Human Normed Mean											1.45
Human Normed Median											0.36

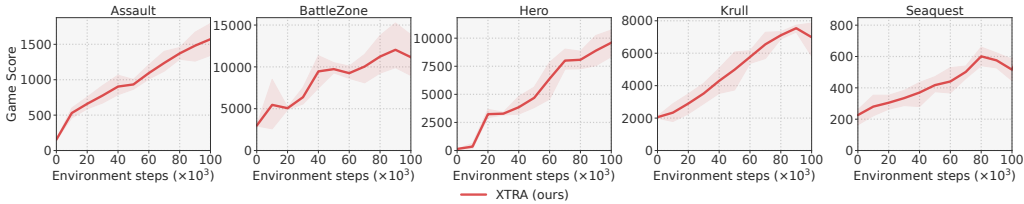


Figure 12. **Atari100k benchmark results (diverse pretraining tasks).** We report unnormalized scores, aggregated across 5 seeds per game. Shaded area indicates 95% confidence intervals.

F ADDITIONAL EVALUATION CURVES OF XTRA ON ATARI100K BENCHMARK

For completeness, Figure 12 includes evaluation curves of XTRA on the five diverse games for which we report final performance in Table 2.

G PER-GAME IMPROVEMENT OVER EFFICIENTZERO

We visualize XTRA’s mean improvement over EfficientZero and EfficientZero-L under similar and diverse task settings on a per-game basis. The improvement is calculated based on the formula: $(\text{score}_{\text{XTRA}}/\text{score}_{\text{Baseline}}) - 1$. The Baseline can be either EfficientZero or EfficientZero-L, depending on the visualization setting.

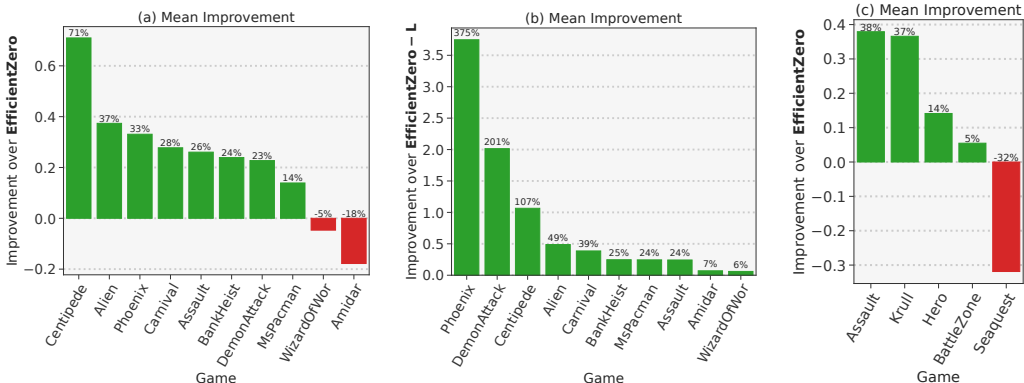


Figure 13. (a) Mean improvement over **EfficientZero** from Table 1 (similar games), (b) Mean improvement over **EfficientZero-L** from Table 1 (similar games), and (c) Mean improvement over **EfficientZero** from Table 2 (diverse games). Each result is aggregated across 5 seeds.

H ARCHITECTURAL DETAILS

We adopt the architecture of EfficientZero (Ye et al., 2021). For EfficientZero-L and XTRA, we increase the number of residual blocks from 1 (default) to 4 (ours) in the representation network, which we find to improve pretraining slightly for XTRA. However, we find that our baseline EfficientZero (without pretraining) performs significantly worse with a larger representation network. Therefore, we use the default EfficientZero as the main point of comparison throughout this work and only include Efficient-L for completeness.

The architecture of the **representation network** is as follows:

- 1 convolution with stride 2 and 32 output planes, output resolution 48x48. (BN + ReLU)
- 1 residual block with 32 planes.
- 1 residual downsample block with stride 2 and 64 output planes, output resolution 24x24.
- 1 residual block with 64 planes.
- Average pooling with stride 2, output resolution 12x12. (BN + ReLU)
- 1 residual block with 64 planes.

- Average pooling with stride 2, output resolution 6x6. (BN + ReLU)
- 1 residual block with 64 planes.

where the kernel size is 3×3 for all operations.

The architecture of the **dynamics network** is as follows:

- Concatenate the input states and input actions into 65 planes.
- 1 convolution with stride 2 and 64 output planes. (BN)
- A residual link: add up the output and the input states. (ReLU)
- 1 residual block with 64 planes.

The architecture of the **reward prediction network** is as follows:

- 1 1x1convolution and 16 output planes. (BN + ReLU)
- Flatten.
- LSTM with 512 hidden size. (BN + ReLU)
- 1 fully connected layers and 32 output dimensions. (BN + ReLU)
- 1 fully connected layers and 601 output dimensions.

The architecture of the **value and policy prediction networks** is as follows:

- 1 residual block with 64 planes.
- 1 1x1convolution and 16 output planes. (BN + ReLU)
- Flatten.
- 1 fully connected layers and 32 output dimensions. (BN + ReLU)
- 1 fully connected layers and D output dimensions.

where $D = 601$ in the value prediction network and $D = |\mathcal{A}|$ in the policy prediction network.

I HYPER-PARAMETERS

We adopt our hyper-parameters from EfficientZero (Ye et al., 2021) with minimal modification. Because XTRA uses data from offline tasks to perform cross-task transfer during online finetuning, we have an additional hyper-parameter for mini-batch size for offline tasks, which is set to 256 (default). We list all hyper-parameters in Table 4 for completeness. Lastly, we note that Ye et al. (2021) performs an additional 20k gradient steps at 100k environment steps, with a $10\times$ smaller learning rate. We follow this procedure when comparing to previous state-of-the-art methods (Table 2), but for simplicity we omit these additional gradient steps in the remainder of our experiments for both XTRA and baselines.

J GAME INFORMATION

In this section, we aim to provide additional context about the games that we consider during both pretraining and finetuning. Table 5 lists core properties for each game. The **Similar Task** column marks all games used in Table 1 (*similar* games), and the two **Diverse Task** columns mark all games used in Table 2 (*diverse* games) for pretraining and finetuning, respectively. We further categorize games into five categories based on game mechanics: *Maze*, *Shooter*, *Tank*, *Adventure*, and *Ball Tracking*, and also report whether the scene is static or dynamic, as well the (valid) action space for each task. The maximum action space for Atari games is 18.

K GAME VISUALIZATIONS

We here provide sample trajectories for each game. These visualizations aim to highlight that (1) it is reasonable to expect some degree of cross-task transfer in *similar* game transfer (maze \rightarrow

Table 4. Hyper-parameters. We list all relevant hyper-parameters below. Values are adopted from Ye et al. (2021) with minimal modification but included here for completeness.

Parameter	Setting
Observation down-sampling	96×96
Frames stacked	4
Frames skip	4
Reward clipping	True
Terminal on loss of life	True
Max frames per episode	108K
Discount factor	0.997^4
Mini-batch size (offline tasks)	256
Mini-batch size (target task)	256
Optimizer	SGD
Optimizer: learning rate	0.2
Optimizer: momentum	0.9
Optimizer: weight decay (c)	0.0001
Learning rate schedule	$0.2 \rightarrow 0.02$
Max gradient norm	5
Priority exponent (α)	0.6
Priority correction (β)	$0.4 \rightarrow 1$
Training steps	100K/120K
Evaluation episodes	32
Min replay size for sampling	2000
Self-play network updating interval	100
Target network updating interval	200
Unroll steps (l_{unroll})	5
TD steps (k)	5
Policy loss coefficient (λ_1)	1
Value loss coefficient (λ_2)	0.25
Self-supervised consistency loss coefficient (λ_3)	2
LSTM horizontal length (ζ)	5
Dirichlet noise ratio (ξ)	0.3
Number of simulations in MCTS (N_{sim})	50
Reanalyzed policy ratio	1.0

Table 5. Game information. We consider a variety of games in our experiments. Here, we provide more context to our selection of games. In our *similar* experiments (Table 1), we finetune model to each game after pretraining it on the other games within the same category. In *diverse* experiments (Table 2), we finetune a single model pretrained on all eight games to each of the target games.

Games	Similar Task (Pretrain & Fine Tune)	Diverse Task (Pretrain)	Diverse Task (Fine Tune)	Category	Static Scene	Action Space
Alien	✓			Maze		18
Amidar	✓			Maze	✓	10
Assault	✓		✓	Shooter	✓	7
Bank Heist	✓			Maze		18
Carnival	✓	✓		Shooter	✓	6
Centipede	✓	✓		Shooter	✓	18
DemonAttack	✓			Shooter	✓	6
MsPacman	✓			Maze		9
Phoenix	✓	✓		Shooter		8
WizardOfWor	✓	✓		Maze		10
BattleZone			✓	Tank	✓	18
Hero			✓	Adventure		18
Krull			✓	Adventure		18
Seaquest			✓	Shooter	✓	18
Pooyan		✓		Shooter		6
Riverraid		✓		Shooter	✓	18
VideoPinball		✓		Ball Tracking		9
YarsRevenge		✓		Shooter		18

maze, shooter \rightarrow shooter) due to similarity in visuals and game mechanics, and (2) that games from our *diverse* category indeed are diverse, both in terms of visuals and mechanics. Figure 14 shows trajectories for five *Maze* games, Figure 15 shows trajectories for five *Shooter* games, and Figure 16 shows trajectories for eight games from our *diverse* game category.

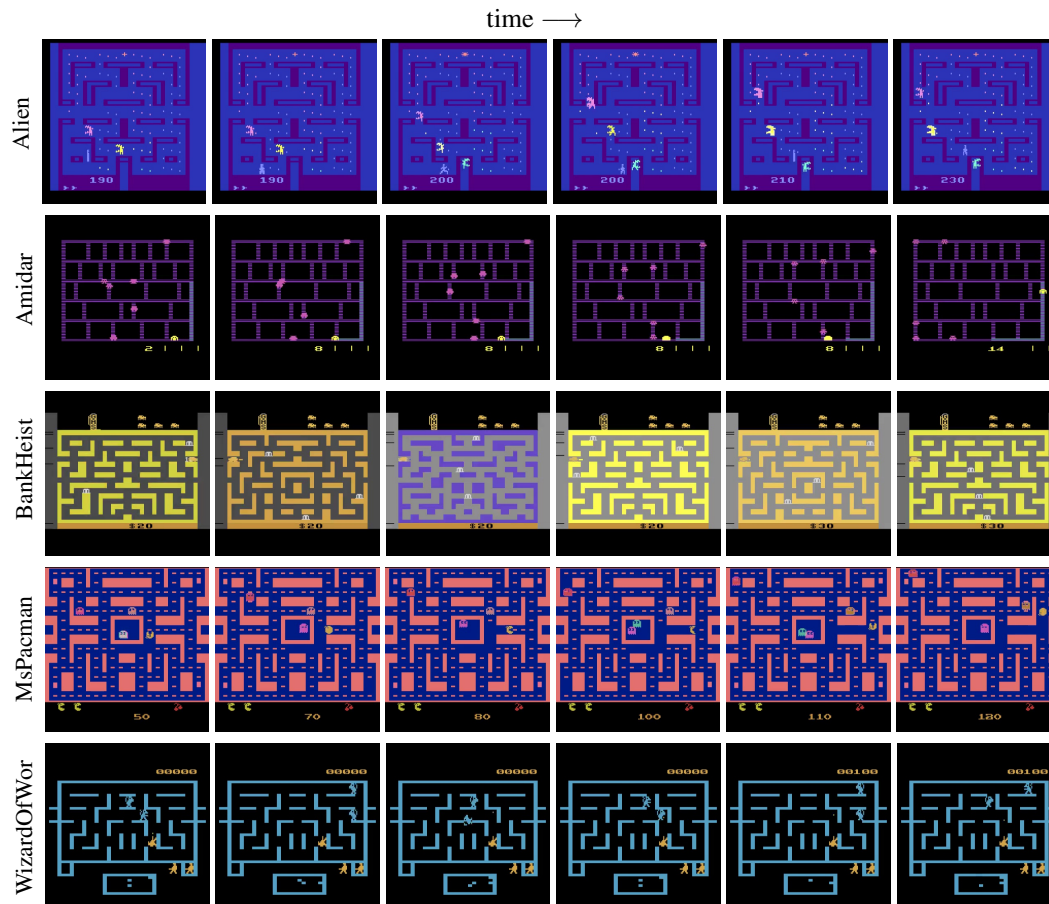


Figure 14. Visualization of trajectories from the Maze game category. We visualize key frames in sample trajectories for five tasks. Actual trajectory lengths vary greatly between games.

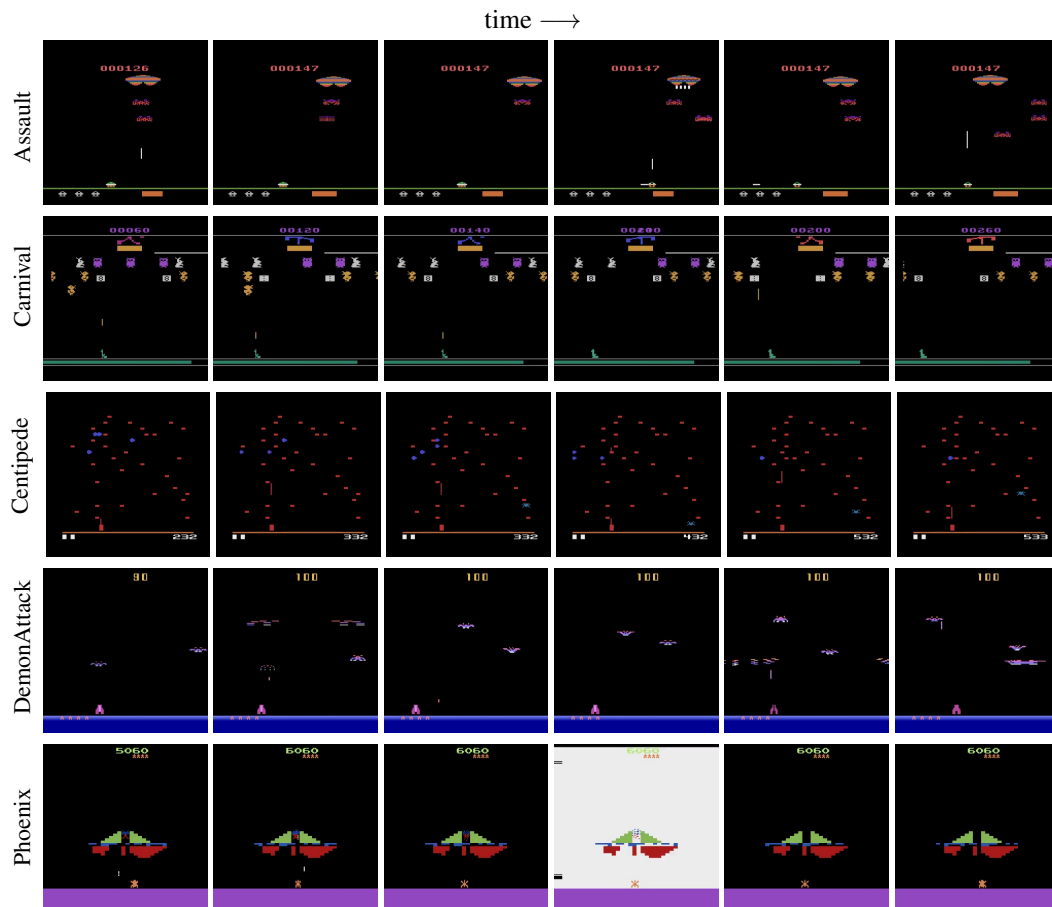


Figure 15. Visualization of trajectories from the *Shooter* game category. We visualize key frames in sample trajectories for five tasks. Actual trajectory lengths vary greatly between games.

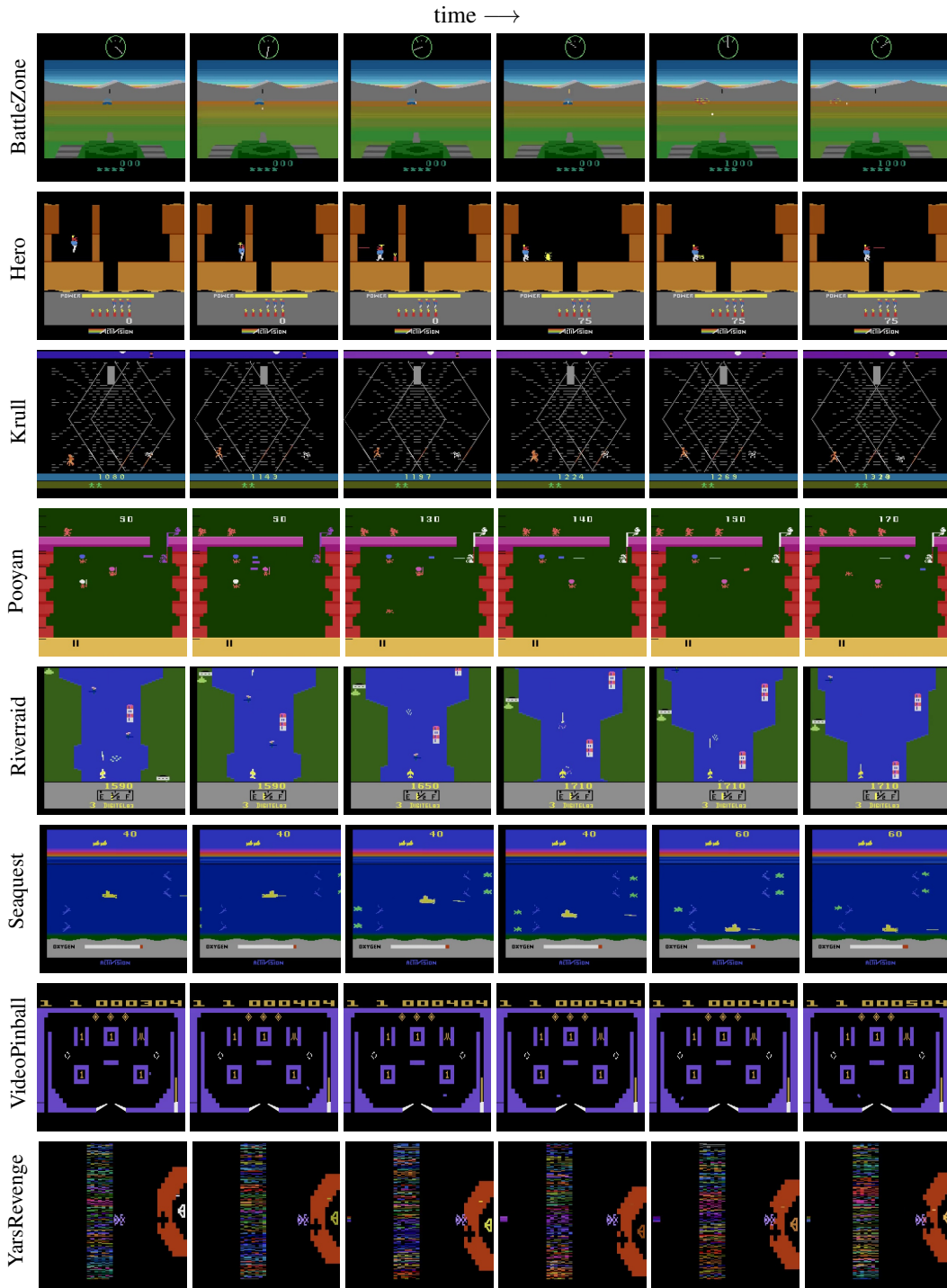


Figure 16. Visualization of trajectories from the *diverse* game category. We visualize key frames in sample trajectories for eight tasks. Actual trajectory lengths vary greatly between games.